JCTC Journal of Chemical Theory and Computation

Article

pubs.acs.org/JCTC

Modeling Proton Dissociation and Transfer Using Dissipative Particle Dynamics Simulation

Ming-Tsung Lee, Aleksey Vishnyakov, and Alexander V. Neimark*

Department of Chemical and Biochemical Engineering, Rutgers, The State University of New Jersey, 98 Brett Road, Piscataway, New Jersey 08854-8058, United States

Supporting Information

ABSTRACT: We suggest a coarse-grained model for dissipative particle dynamics (DPD) simulations of solutions with dissociated protons. The model uses standard short-range soft repulsion and smeared charge electrostatic potentials between the beads, representing solution components. The proton is introduced as a separate charged bead that forms dissociable bonds with proton receptor base beads, such as water or deprotonated acid anions. The proton−base bonds are described by Morse potentials. When the proton establishes the Morse bonds with two bases, they form an intermediate complex, and the proton is able to "hop" between the bases artificially mimicking the Grotthuss diffusion mechanism. By adjusting the Morse potential parameters, one can regulate the potential barrier associated with intermediate complex formation and breakup and control the hopping frequency. This makes the proposed model applicable to simulations of proton mobility and reaction equilibria between protonated and deprotonated acid forms in aqueous solutions. The proposed model provides quantitative agreement with experiments for the proton self-diffusion coefficient and hopping frequency, as well as for the degree of dissociation of benzenesulfonic acid.

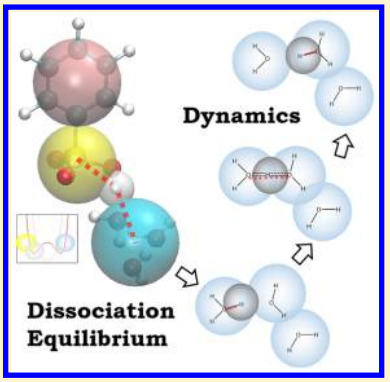

I. INTRODUCTION

Dissipative particle dynamics (DPD) simulations[1] have become a powerful tool to study complex fluids and soft matter on spatial and temporal scales that cannot be accessed on the quantum or atomistic levels. In the common implementations of DPD, the molecules of interest are dissected into the fragments of approximately equal volume. The atoms of each fragment are lumped together and represented by a spherical quasi-particle ("bead"); the beads interact via short-range soft repulsion potentials. This approach provides a superb computational efficiency. The price to pay for that is a crudeness of coarse-grained models, and therefore a limited range of phenomena to which DPD simulations can be applied to achieve quantitative results. Nevertheless, with recent advances, DPD simulations are targeting systems of increasing complexity that involve long-range electrostatic interactions, such as charged biopolymers[2] and segregating polyelectrolytes.[3]

Segregation in polyelectrolytes is especially challenging, because it involves a redistribution of charged species far beyond the molecular scale. The dissociation of a particular counterion is determined by the local environment around it rather than by macroscopic properties, such as pH. Therefore, it is desirable that the dissociation be embedded directly into the simulation force field. In published DPD studies of polyelectrolytes, dissociation/association of counterions was considered indirectly. The pioneering DPD studies of polyelectrolytes[4] did not explicitly involve ions, effectively replacing long-range electrostatic interactions with short-range ones. Explicit introduction of electrostatics into DPD via the smeared charge approach, combined with the Ewald method[5] or PPPM,[6] allowed simulations to be performed with a fixed degree of dissociation or fixed fractional charges assigned to dissociating groups. For example, in our recent DPD simulations[3d] of metal-substituted Nafion polymer at low water content, the dissociation degree was fixed and the respective fraction of the alkali metal counterions were considered to be dissociated from their sulfonate groups and represented by hydrated counterion beads; the rest of the counterions were kept attached to the side chains, and such pair were modeled by neutral beads. This approach, which avoids modeling dissociation equilibrium, is suitable for strong acid−base pairs (e.g., fluorinated sulfonic acid and alkali metals), yet it is hardly applicable in the case of weaker acids. In fact, the dissociation degree in ref 3d was determined by the coarse graining scheme, rather than by chemical considerations. Alternatively, each dissociating group may be assigned a fractional charge according to a degree of dissociation calculated theoretically. This approach was employed in DPD simulations of α-synuclein that contains both carbonic acid and amine groups.[2a] The net charge was compensated by explicit ions. However, the applicability this approach is limited to the systems where the dissociation degree can be reliably predicted (e.g., to dilute electrolyte solutions).

The second class of problems that may require explicit consideration of dissociating ions is related to their transport in

Received: May 20, 2015
Published: July 28, 2015

DOI: 10.1021/acs.jctc.5b00467
J. Chem. Theory Comput. 2015, 11, 4395−4403

complex geometries, such as proton exchange ionomers of which Nafion is the best-known example. The mechanisms of proton mobility in such environments include the Grotthuss-type "hopping" that involves formation of various proton−water complexes like hydronium (H_3O^+), Zundel ($H_5O_2^+$), and Eigen ($H_9O_4^+$) ions, as well as proton−water−sulfonate complexes. In the literature, the hopping mechanisms were considered in an indirect manner. Jorn and Voth[3a] modeled the nanostructure of segregated polymer with standard short-range DPD potentials, and then considered proton transport in the structures obtained using smoothed particle hydrodynamics (SPH).[7] Transport coefficients and coarse-grained forces for the polymer backbone, side chain, proton, and water interactions were derived from molecular dynamics (MD) simulations. The proton conductance profiles determined in this simulation at the 40 nm scale are in semiquantitative agreement with results of earlier experiments.[8] The authors also showed that accounting for the electrostatic interactions is crucial for the improvement of proton transport modeling with DPD.

Accurate representation of the formation and breakup of proton−water and proton−water−anion structures poses a serious challenge, even in classical MD. Several approaches to incorporating proton transfer into classical MD were proposed, most of which were aimed at modeling proton diffusion in ion-exchange membranes.[9] Nevertheless, reactivity has been included in coarse-grained models of polymers. Lisal et al.[10] considered polymerization in polymer melts using DPD simulations. Protonation was included via Monte Carlo (MC)-like steps that involve bond formation and dissociation.[11] Formation and breakup of temporary bonds was considered also by Karimi-Varzaneh et al.,[12] with a purpose of mimicking polymer chain entanglements in polymer solutions and melts. By incorporating the theoretically informed coarse graining approach[13] into DPD, Nikoubashman et al.[14] studied block copolymer thin films, where the essential properties (such as chain connectivity) were preserved. Although these authors did not target reactivity (rather, they succeeded in describing polymer melt viscosity with soft-core models), their approach is relevant to reactive systems as well.

In this paper, we suggest a mesoscale simulation framework that directly incorporates dissociation−association of proton−base complexes into the DPD force field. We specifically address the proton mobility in the water and protonation equilibria in the solution of acids by artificially mimicking Grotthuss-type mechanisms of formation and breakup of the proton−water and proton−anion (such as deprotonated acid) complexes. In Section II, we briefly review the theoretical scheme of DPD and the smeared charge approximation adopted in this work. Section III presents the proposed model of proton transport within the DPD scheme. The proton is introduced as a separate charged bead that forms dissociable bonds with proton receptive base beads, such as water or deprotonated acid anions. The proton−base bonds are described by Morse potentials. When the proton established Morse bonds with two bases, they form an intermediate complex, and the proton is able to "hop" between the bases artificially mimicking the Grotthuss diffusion mechanism. We explain how the interaction of model proton with different bases and formation of the proton-base complexes are controlled by the Morse potential. In Section IV, we apply the proposed framework to modeling the proton mobility in water. In Section V, we study the equilibrium properties of dilute solutions of benzenesulfonic acid. Conclusions are summarized in Section VI.

II. DPD SIMULATIONS

The system under consideration is presented as multicomponent mixture of beads with an equal effective diameter R_C. Four types of beads are involved in simulations: deprotonated benzenesulfonic acid is represented by a dimer of bead C (C_5H_5) and bead S (CSO_3^-) connected by a harmonic bond. Proton (H^+) is modeled as a charged bead P described in Section III. Water bead W either includes a single H_2O molecule ($N_W = 1$; this model is used in simulations of proton mobility) or three H_2O molecules ($N_W = 3$). This bead size is chosen due to coarse graining of benzenesulfonic acid; dissociation of which is considered in Section V. The system dynamics and equilibrium are studied by solving Newton equations of motions with pairwise interbead forces given in eq 1.

$$\mathbf{F}_{ij}(\mathbf{r}_{ij}) = \mathbf{F}_{ij}^{(C)}(\mathbf{r}_{ij}) + \mathbf{F}_{ij}^{(D)}(\mathbf{r}_{ij}, \mathbf{v}_{ij}) + \mathbf{F}_{ij}^{(R)}(\mathbf{r}_{ij}) + \mathbf{F}_{ij}^{(B)}(\mathbf{r}_{ij}) + \mathbf{F}_{ij}^{(E)}(\mathbf{r}_{ij}) + \mathbf{F}_{ij}^{(M)}(\mathbf{r}_{ij}) \quad (1)$$

The short-range conservative repulsive force $\mathbf{F}_{ij}^{(C)}$ acts between overlapping beads: $\mathbf{F}_{ij}^{(C)}(\mathbf{r}_{ij}) = a_{IJ}w(r_{ij})\mathbf{r}_{ij}/r_{ij}$, where $w(r_{ij}) = 1 - r_{ij}/R_C$ for $r_{ij} < R_C$ and $w(r_{ij}) = 0$ for $r_{ij} \geq R_C$; a_{IJ} is the repulsion parameter specific to the given bead pair of types I and J. The intracomponent repulsion parameters between beads of the same type are set equal, irrespective of the bead type (i.e., $a_{JJ} = a_{II}$). The intercomponent repulsion parameter for C−W pair type is determined from the reference compound solubility, similar to ref 15. The beads are packed at the standard[16] reduced density $\rho R_C^3 = 3$.

The random and drag force institute the Langevin thermostat; they act between the overlapping beads along the line connecting the bead centers. The drag force is velocity-dependent: $\mathbf{F}_{ij}^{(D)}(\mathbf{r}_{ij},\mathbf{v}_{ij}) = -\gamma w(r_{ij})^2(\mathbf{r}_{ij}*\mathbf{v}_{ij})$, where $\mathbf{v}_{ij} = \mathbf{v}_j - \mathbf{v}_i$ ($\mathbf{v}_i$ and $\mathbf{v}_j$ are the current velocities of the particles). The random force $\mathbf{F}_{ij}^{(R)}$, which accounts for thermal fluctuations, is taken to be proportional to the conservative force: $\mathbf{F}_{ij}^{(R)}(\mathbf{r}_{ij}) = \sigma w(r_{ij})r_{ij}\theta_{ij}(t)\mathbf{r}_{ij}/r_{ij}$, where $\theta_{ij}(t)$ is a variable that randomly fluctuates in time with Gaussian statistics. The fluctuation−dissipation relationship couples the noise level σ and friction factor γ that $\sigma^2 = 2\gamma kT$.[17] The parameter is set as $\gamma = 4.5$, which is a suggested value for a better simulation temperature control.[16] In the model of benzenesulfonic acid, the hydrophobic benzene ring C and the hydrophilic sulfonate group S are connected by a harmonic bond $\mathbf{F}_{ij}^{(B)}(\mathbf{r}_{ij}) = K_B(r_{ij} - r_0)\mathbf{r}_{ij}/r_{ij}$, where r_0 is the equilibrium bond length and K_B is the bond rigidity, which is dependent on the bead type.

The long-range electrostatic force $\mathbf{F}_{ij}^{(E)}$ between P and S beads, representing charged species, is implemented using the smeared charge approach.[5] Instead of point charges, the charge is modeled as a symmetric cloud around the bead center. Charge smearing avoids the divergence of electrostatic potential at $r_{ij} \to 0$ and allows for integration of the equations of motion with a long time step that is the main advantage of DPD. Linear,[6,18] exponential,[5] Gaussian-type,[19] and Bessel-type[20] decays of charge density were attempted in the literature. In this work, we use a Slater-type smearing model, described by Gonzales-Melchor et al.,[5] where the charge distribution is $f(r) = (qe/\pi\lambda^3)\exp(-2r/\lambda)$, and λ is the effective smearing length chosen as $0.25R_C$ to all charged beads (see detailed discussions

DOI: 10.1021/acs.jctc.5b00467
J. Chem. Theory Comput. 2015, 11, 4395−4403

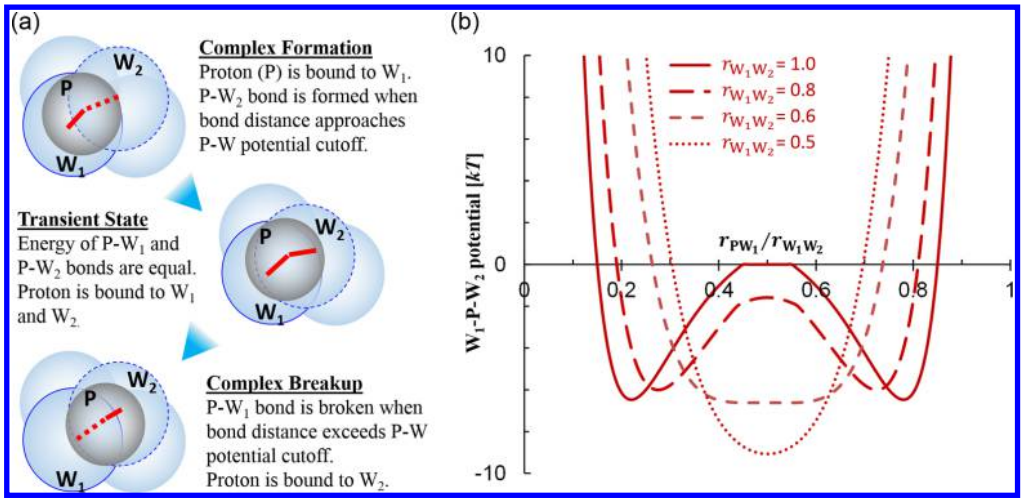

Figure 1. (a) Schematics of the coarse-grained model of the proton (P) transfer between two water beads W_1 to W_2 through the formation and breakup of an intermediate complex W_1−P−W_2. The radius of the P bead depicts the P−W Morse potential cutoff, and the red bars are effective P−W bonds (solid line denotes strong bonding, dashed lines represent weak bonding). (b) Potential energy of the W_1−P−W_2 complex along the proton transfer reaction coordinate. The energy profile has two potential minima, and the transfer is associated with an energy barrier, crossing of which mimics the proton hopping. The energy profiles are given for $N_W = 1$, $a_{WW} = 23.4kT/R_C$, $K_{PW} = 8.5$, $\alpha_{PW} = 2$, $r^0_{PW} = 0.22R_C = 1$ Å, and $r^M_{PW} = 0.45R_C = 2$ Å.

in section S1 in the Supporting Information). The electrostatic force $\mathbf{F}^{(E)}_{ij}$ between charged particles i and j in eq 1 is expressed as

$$\mathbf{F}^{(E)}_{ij}(\mathbf{r}_{ij}) = \frac{e^2 q_i q_j}{4\pi kT\varepsilon_0\varepsilon_r R_C r_{ij}^2} \times\left[1 - \exp\left(-\frac{2R_C r_{ij}}{\lambda r_{ij}}\right)\left(1 + \frac{2R_C r_{ij}}{\lambda(1 + R_C r_{ij}/\lambda)}\right)\right]\frac{\mathbf{r}_{ij}}{r_{ij}} \quad (2)$$

At long range, the electrostatic interaction of smeared charges (eq 2) reduces to the Coulomb potential and the standard Ewald summation[21] is used to account for the periodic boundary conditions.

The last term $\mathbf{F}^{(M)}_{ij}(\mathbf{r}_{ij})$ in eq 1 represents the Morse bond that accounts for the formation of dissociative complexes between proton bead P and base beads W and S. The details of the Morse bond implementation and parametrization are described below in Section III.

Simulations are performed by DL_MESO DPD package[22] with the original implementation of the pairwise Morse bonds. The computational details are given, together with the results of simulations in Sections IV and V.

III. COARSE-GRAINED MODEL OF PROTONS

To introduce protons into the DPD framework, we employ a concept similar to that used in reactive MD.[11a,23] We use a proton bead P, which bears a positive charge ($+e$) and has a mass equal to $1/(18N_W)$ of the water bead mass. (N_W is the number of water molecules in one water bead.) Proton bead P is allowed to form dissociable bonds with the proton-receptive beads, which we call base beads, such as the neutral water bead (W) and the charged sulfonate (CSO_3^-) bead (S). Proton bead P experiences no short-range repulsion $\mathbf{F}^{(C)}$ with the bases, but may repel from other beads. The dissociable bonds are modeled by the Morse potential $U^{(M)}_{ij}$ cut and shifted to zero at the cutoff distance r^M,

$$U^{(M)}_{ij}(r_{ij}) = K_{IJ}\{1 - \exp[\alpha_{IJ}(r_{ij} - r^0_{ij})]\}^2 - K_{IJ}\{1 - \exp[\alpha_{IJ}(r^M_{ij} - r^0_{ij})]\}^2 \quad (3a)$$

and the Morse force is given by

$$\mathbf{F}^{(M)}_{ij}(\mathbf{r}_{ij}) = -2\alpha_{IJ}K_{IJ}\exp[\alpha_{IJ}(r_{ij} - r^0_{ij})]\{1 - \exp[\alpha_{PB}(r_{ij} - r^0_{ij})]\}\frac{\mathbf{r}_{ij}}{r_{ij}} \quad \text{at } r_{ij} < r^M_{ij} \quad (3b)$$

The Morse potential (eq 3a) has a minimum at $r_{ij} = r^0_{ij}$ and is characterized by the strength parameter K_{IJ} and the effective steepness α_{IJ}. When $r_{ij} \approx r^0_{ij}$, the Morse potential is similar to the harmonic potential with effective stiffness K_{IJ}. Because the potential is cut and shifted, the overall depth does not equal K, but rather is dependent on K, α, and r^M and is denoted as E^M. This attractive force keeps the proton in the "associated" state, making it fluctuate around a particular base bead. The force is repulsive when $r_{ij} < r^0_{ij}$. Thus, the proton does not entirely "belong" to any host base, but the Morse interactions with overlapping base beads make its stand-alone existence apart from a base improbable especially in the densely packed DPD fluid.

Figure 1a illustrates the proton transfer between two water beads, W_1 and W_2, in the DPD model. Initially, the proton bead P is associated with W_1 by P−W_1 Morse bond. When another base W_2 appears within the P−W Morse potential cutoff, an intermediate complex W_1−P−W_2 is formed. The potential energy of the intermediate shown in Figure 1b is the sum of the repulsion potential between water beads W_1 and W_2 and the two Morse potentials of P−W_1 and P−W_2 bonds. The potential energy profile has two minima along the reaction coordinate $r_{PW_1}/r_{W_1W_2}$. (The P bead is assumed to be located on the line connecting the centers of water beads.) The two minima are divided by a potential barrier associated with possible activated hopping of proton from W_1 to W_2. The minima merge when the distance between the water beads becomes shorter, effectively creating a single potential well. When the W_1−W_2 distance increases again due to thermal fluctuations, the proton

DOI: 10.1021/acs.jctc.5b00467
J. Chem. Theory Comput. 2015, 11, 4395−4403

may either migrate from W_1 to W_2 or remains with W_1 after two water beads are separated later.

The same schematics hold for the proton transfer between any pair of base beads, which may be either neutral or charged. Neutral base beads may represent proton-accepting solvent molecules such as water, ammonia, etc. (one bead can represent one or several solvent molecules). Charge base beads are commonly acid anions. In the latter case, the potential energy is augmented by the electrostatic attraction, which favors association. Therefore, the proposed model mimics proton transfer in a solvent bath and allows for equilibrium between protonated and deprotonated forms of acids in solutions. In the latter case, one of the water beads in Figure 1 should be replaced by the anion bead S. Below, we address both equilibrium and dynamic aspects of protonation.

IV. SIMULATIONS OF PROTON DYNAMICS IN WATER

Formation and breakup of intermediate complexes formed by proton P bead and two or more base beads allow one to mimic proton transfer from one base to another. By adjusting the depth and range of proton-base Morse potential, we can adjust the height of the potential barrier associated with the transfer of P bead between base beads, thus reproducing *proton dynamics*. Here, we consider a dilute aqueous solution, where the proton transport is controlled by proton transfer between water molecules (hopping mechanism) and diffusion of proton−water complexes (vehicular mechanism).

Simulations are performed as follows. One P bead is placed in the periodic cubic box of size $20R_C$ filled with 24 000 W beads (bead density of $\rho R_C^3 = 3$). W beads interact with each other by standard DPD repulsion potentials. We consider two coarse-graining levels: $N_w = 1$ (that is, one DPD bead models a single water molecule) and $N_w = 3$ (three water molecules per bead). From the density and compressibility of water liquid under ambient conditions,[24] for $N_w = 1$, we obtain $R_C = 4.45$ Å and $a_{WW} = 23.5kT/R_C$. For $N_W = 3$, $R_C = 6.45$ Å and $a_{WW} = 78kT/R_C$. W beads interact with the P bead only via the Morse potential. Since we address only very dilute solutions here, counterions are not considered and electrostatic interactions are not essential. The length of each simulation was 1 million steps and the reduced step length is 0.01τ, where τ is the dimensionless time unit in DPD. The self-diffusion coefficients of P and W beads are calculated in a standard manner from mean square displacements (MSDs) via the Einstein relationship. Because of a limited ability of DPD to reproduce the dynamic properties of liquids,[16] we do not attempt to reproduce the self-diffusion coefficient of the proton (D_P) *per se*, but rather its ratio to the self-diffusion coefficient of bulk water (D_W) determined in the same simulation, D_P/D_W.[25] Since the mobilities are compared to the experimental self-diffusion coefficients of water, we follow the literature approach[24] to convert the DPD time unit τ to physical time. By matching the MSD of the W bead to the water self-diffusion coefficient (details are discussed in Section S2 in the Supporting Information), we obtain $\tau = 6.8$ ps for $N_W = 1$ and 10.4 ps for $N_W = 3$ with the simulation setup described in this work. Note that, for $N_W > 1$, the apparent diffusion coefficient calculated from the MSD of W beads is N_W times lower than the self-diffusion of water molecules, as discussed in ref 24. Figure 2 shows the MSD of W bead (bulk region) and the P bead in the physical units.

At $N_W = 1$, the W bead contains only one water molecule, the P−W complex effectively corresponds to the hydronium ion (H_3O^+), and the W−P−W complex corresponds to the Zundel ion ($H_5O_2^+$). Proton transfer in this case has a direct atomistic analogue: the formation of the Zundel complex from the hydronium ion and water is followed by its breakup, resulting in a successful or failed attempt of the proton transfer (Figure 1). On the atomistic modeling level, a similar scheme was implemented by Walbran et al.[9c] As a consequence of coarse graining, the DPD model of hydronium has only one P bead, while a real hydronium ion has three equivalent protons, each of which can be involved in the formation of the Zundel ion with a neighboring water molecule. The "fixed" nature of the proton bead does not allow larger complexes such as the Eigen ion ($H_9O_4^+$) with $N_w = 1$. The P bead moves in the solvent bath via a trajectory of interdigitating W−P ("hydronium") and W−P−W ("Zundel") configurations. In the W−P state, the proton, because of its low mass, experiences fast fluctuations around the hosting water bead before it forms a new Morse bond. We choose Morse parameters to reproduce (1) the number of W beads neighboring given P bead (that is, the W beads that simultaneously form Morse bonds with the same P bead), (2) P−W bond lifetime, (3) experimental D_P/D_W ratio (proton self-diffusion in dilute solutions is ∼4 times faster than that of bulk water under ambient conditions[25]).

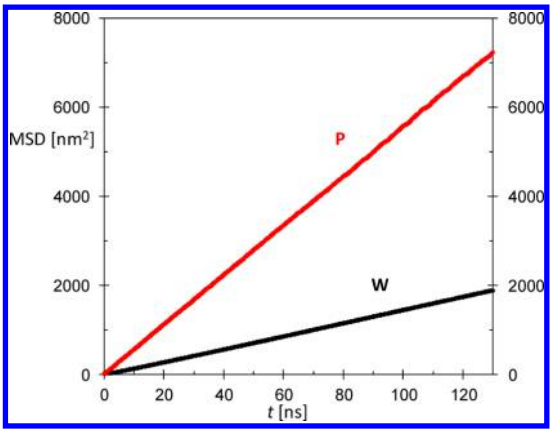

Figure 2. Mean square displacement (MSD, in nm^2) of proton bead (P) and bulk water bead (W) versus simulation time (ns). The ratio of the slopes between P and W in the figure is ∼3.9. Parameters used here are the same as in Figure 1b.

In order to mimic the geometrical parameters of actual hydronium and Zundel complexes, we set the equilibrium P−W bonds distance at $r^0_{PW} = 1$ Å. The reasonable range for Morse cutoff r^M_{PW} is determined from the general definition of hydrogen bond, where the donor−acceptor distance (in this case, it is the distance between two W beads connected to the same P bead) ranges from 2 Å to 4 Å.[26] This condition is satisfied only at relatively short r^M_{PW}; here, we chose $r^M_{PW} = 2$ Å. These parameters also give a reasonable estimate for the activation energy of the P bead transfer between the neighboring W beads. The characteristic distance between the nearest-neighbor beads in the DPD fluid corresponds to the first maximum of the radial distribution function that is $\sim 0.83R_C$. The barrier for the transition of the P bead from its current host to the neighboring one is $4.3kT$, which is very close to the experimental proton transfer activation energy in bulk water at room temperature (0.1 eV).[27] Figure 3 shows the distribution of distance between two W beads connected by Morse bonds to the same P bead at $K_{PW} = 8.5$ and $\alpha_{PW} = 2$. The most probable distance between the basic W−P−W complex is

DOI: 10.1021/acs.jctc.5b00467
J. Chem. Theory Comput. 2015, 11, 4395−4403

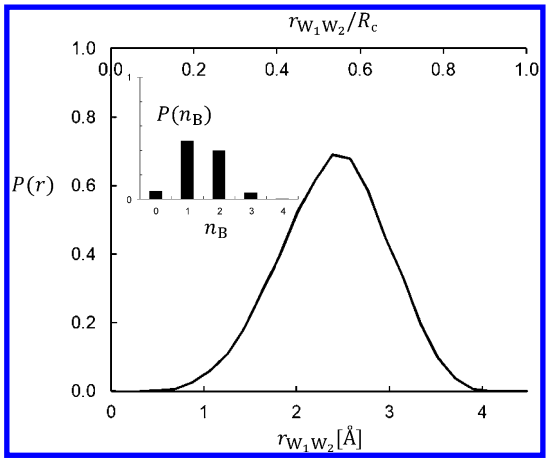

Figure 3. Distribution of distances between two beads W_1 and W_2 in the W_1−P−W_2 complexes. Parameters used here are the same as in Figure 1b. The most probable distance of W_1 and W_2 is 2.4 Å, similar to the oxygen−oxygen distance in the Zundel complex. Inset shows the distribution of the number of P−W bonds.

~2.5 Å. This is very close to the actual distance between two water oxygens in a Zundel complex and to the O−O distance in the water wire (2.5−2.6 Å)[25b] and demonstrates the existence of Zundel-like structures in our DPD simulations. The distribution decays to zero at ~4 Å, which, as we noted above, corresponds well to the actual maximum hydrogen bonds length in associating liquids. The insert on the figure shows the distribution of the number of bonds made by one proton at the same time. The proton mostly connected to one or two water beads, which corresponds to the hydronium-like and Zundel-like states. If r_{PW}^{M} increases, the P bead may establish the Morse bonds with multiple neighboring water beads, yet without identifiable hopping events.

Once r_{PW}^{M} is fixed, the strength of the P−W Morse bond (that is, the actual depth of the Morse potential) determines the lifetime of the hydronium-like and Zundel-like configurations and, therefore, determines the hopping frequency and self-diffusion. For cut-and-shifted version of the Morse potential, the overall depth E_M determines the entire attractive part of the potential (this shortcoming of the chosen type of the dissociating bond is discussed in Section V). The deeper the P−W Morse potential well, the slower P bead moves in the water bath. By scanning the overall depths from $-0.5kT$ to $-50kT$, we found that the sought proton mobility is achieved when $E^M \approx -1.2$. To impose a stronger repulsion between the P and W beads at short distances, we chose a maximum value of the steepness parameter α in eqs 3 that does not compromise the computational efficiency. The parameters employed in this work are given in Table 1.

With these parameters, we obtained the proton mobility that exceeds the water mobility by the factor of $D_P/D_W = 3.8$, which is very close to the experimental data. The P bead moves in the W bath via a series of "hops". We characterize the frequency of hopping events using a "hosting time" t_h. The hosting time is a period between two consecutive hopping events. The hosting time for our DPD model is ~2.6 ps, which agrees very reasonably with the experimental data of 2.0 ps. The average lifetime of a hydronium-like formation is 1.7 ps, and that for the Zundel-like formation is 1.4 ps.

A coarser representation of water ($N_W = 3$) results in a higher repulsion parameter a_{WW}, more structured fluid, and lower degree of overlap between water beads. The proton is introduced similarly to the monomolecular model with $N_W = 1$; P bead that forms dissociable Morse bonds to W bead and can be transfer between them, according to the schematics shown in Figure 1. The main difference is that the actual proton modeled by P bead can be transferred between the water molecules that effectively belong to the same W bead. Therefore, there is no geometrical reason to introduce Morse repulsion between W and P beads. We decided to set the equilibrium P−W distance r_{PW}^{0} in eq3b to zero. The removal of the repulsion part of the Morse potential at $r_{PW} < r_{PW}^{0}$ allows the P bead to reside near the center of its host base. Therefore, the distance between the minima of potential energy for an individual act of proton transfer (Figure 1) increases, the number of Morse bonds formed concurrently via the same P bead decreases, which leads to slower transfer rates. However, the increasing ratio of W and P bead weight creates more distinct velocity differences of the P bead and the W bead, requiring a stiffer P−W potential to reach the target D_P/D_W ratio. The dependence of overall proton mobility and P−W parameters follows the same trend as in the monomolecular model discussed above. The P−W potential, which reproduces proton mobility in bulk water, is used in the following section. The potential parameters obtained, following the same approach as that for the monomolecular model, are listed in Table 1.

Table 1. Parameters of DPD Models: (A) Morse Parameters for P−W Potential (eqs 3), Which Reproduce Experimental Proton Mobility ($D_P/D_W \approx 4$), (B) Interbead Repulsion Parameters for Modeling Benzenesulfonic Acid Solution ($N_W = 3$), and (C) Bond Parameters for Modeling Benzenesulfonic Acid Solution ($N_W = 3$)

(A) Morse Parameters

bead size	a_{WW} (kT/R_C)	K_{PW}	r_{PW}^{0} (Å)	α_{PW}	r_{PW}^{M} (Å)	depth of the P−W Morse potential, E_M (kT)
$N_W = 1$, R_C = 4.48 Å	23.4	8.5	1	2	2.0	−1.2
$N_W = 3$, R_C = 6.46 Å	78.5	16.0	0	1	3.9	−3.3

(B) Short-Range Repulsion Parameters, $(a_{IJ}R_C)/kT$ ($N_W = 3$)

	W	S	C	P
W	78.5	78.5	91.2	0.0
S	78.5	78.5	78.5	0.0
C	91.2	78.5	78.5	91.2
P	0.0	0.0	91.2	0.0

(C) Bond Parameters

bond/type	K	r^0 (Å)	α	r^M (Å)	E_M (kT)
C−S (harmonic)	200.0	5.2			
P−W (Morse)	16.0	0.0	1	3.9	−3.3
P−S (Morse)	18.5	2.2	2	4.2	−4.2

V. MODELING OF REACTION EQUILIBRIUM: DEPROTONATION OF BENZENESULFONIC ACID

As a representative example, we chose benzenesulfonic acid aqueous solution, because polymers that contain phenylsulfonic acid groups are commonly used in proton-exchange membranes; these are systems that have particular practical interest. An analogy between the atomistic and DPD models is shown in Figure 4.

DOI: 10.1021/acs.jctc.5b00467
J. Chem. Theory Comput. 2015, 11, 4395−4403

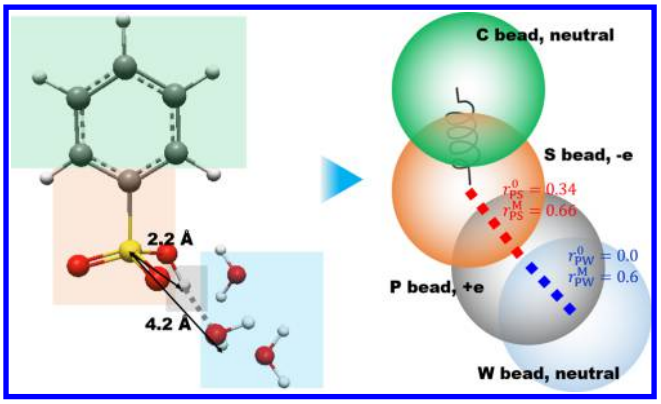

Figure 4. Coarse-grained representation of benzenesulfonic acid (sulfur in yellow, oxygen in red). Colored blocks on the atomistic model denote the fragments that constitute the respective DPD beads. The coarse-graining level corresponds to three water molecules per bead. C−S dimer represents the deprotonated acid ion. The equilibrium distance and the cutoff of the associative harmonic potential between beads S and P are chosen from the *ab initio* calculations. (See Section S3 in the Supporting Information.)

The coarse-graining level of $N_W = 3$ and $R_C = 6.65$ Å is dictated by the chosen dissection of the benzenesulfonate anion ($C_6H_5SO_3^-$) into two beads of the comparable size. Note that the presence of dissociating species other than small solvent molecules limits the choice of N_w. In particular, $N_w = 4$ would be a convenient coarse-graining level for water, since the protonated water bead could effectively represents an Eigen ion. However, acid groups (such as sulfonate) are typically rather small. If such a group was included in a bigger bead, the same bead would have to contain hydrophobic fragments or associated water that might be undesirable. The coarse-graining level chosen here ($N_w = 3$) is very common in DPD simulations of surfactants.[24] According to our calculation with the COSMO model[28] performed with PQS software,[29] the volume of the benzenesulfonate anion is ∼6 times as large as that of a water molecule (recall Section S3). Therefore, we model benzenesulfonate as a dimer composed of a neutral hydrophobic C bead and a negatively charged hydrophilic S base bead. The beads are connected by a stiff harmonic bond at an equilibrium length equal to $0.8R_C$ with a bond stiffness of $K_B = 200kT/R_C^2$. Following the standard DPD formulation,[24] the intracomponent repulsion parameter $a_{II} = 78.5kT/R_C$ was assigned for all bead types. Intercomponent parameters between acid and water play no significant role in dilute solutions (0.01−0.09 M) considered here, since acid molecules are well dissolved in the solution with no aggregation. Parameter for hydrophobic component $a_{CW} = 91.2kT/R_C$ was estimated from benzene solubility in water, using the approach suggested in our previous work.[15] Parameter a_{SW} was set to zero.

The sulfur atom is the geometric center of the CSO_3^- fragment represented by the S bead. Naturally, the S−H distance observed in benzenesulfonic acid molecule serves as the equilibrium distance r_{PS}^0. The interaction between sulfonate and proton may be reduced to electrostatic attraction if the proton is separated from the anion by water oxygen. This distance was chosen as the Morse bond cutoff. It was estimated with the DFT optimization of $C_6H_5{-}SO_3H{\cdot}3H_2O$ clusters described in Section S3 as $r_{PS}^M = 0.66R_C$.

The P bead experienced no short-range repulsion from W and S beads ($a_{PW} = a_{PS} = 0$); however, a repulsion parameter of $a_{CP} = 91.2kT/R_C$ was assigned in order to avoid proton bead from overlapping with the benzene ring. The P bead interacts with the acid anion S bead via electrostatic interaction, as well as via the Morse bond, provided that $r_{PS} < r_{PS}^M$. The existence of the Morse bond serves as a criterion that P and S beads are associated. The equilibrium and cutoff distance parameters for P−S Morse bonds were assigned from geometric considerations, based on the distance from S atom to associate proton and to the H atom on the associated water molecule. (See Table S3 in the Supporting Information.) At the same time, the P bead may form Morse bonds with the surrounding water W beads. The parameters of P−W Morse potential listed in Table 1 were determined to provide quantitative agreement with the experimental proton mobility, as described in the previous section.

Dissociation of benzenesulfonic acid is presented as a reaction: CSP + W ⇌ CS + WP, characterized by the equilibrium constant $K_a \approx [CS][WP]/[CSP]$. This approximation holds for dilute solutions, where the dependence of activity coefficients on concentration may be neglected. The experimental dissociation constant K_a for benzenesulfonic acid is 0.2. The dependence of the degree of dissociation on the total concentration of sulfonate may be calculated as described by eq 4, the derivation of which has been derived in Section S4 in the Supporting Information:

$$\beta = \frac{[CS]}{[CSP]_0} = \frac{-K_a + \sqrt{K_a^2 + 4K_a[CSP]_0}}{2[CSP]_0} \quad (4)$$

The DPD simulations of protonation equilibrium were performed in a $30 \times 30 \times 30R_C^3$ simulation box containing a total of 81 000 DPD beads over 500 000 DPD time steps of $0.01(kT/m)^{-1/2}R_C$. After 100 000 steps for equilibration, the degree of dissociation was calculated as a fraction of S beads that formed no Morse bonds with any of the P beads at a given moment, i.e., $r_{PS} > r_{PS}^M = 4.2$ Å. Noteworthy, the electrostatic interactions alone are insufficient for describing CS protonation: the calculated degrees of dissociation was close to 1 in all systems with $K_{PS} = 0$. Although the electrostatics with the short decay length (eq 2) provides $-4kT$ when P and S beads are fully overlapped (as determined using the integral of eq 2 at $r = 0$), the P bead prefers being hosted by the W bead ($-3.3kT$), which is repelled from the S bead. Temporary association of the P and S beads is due to the rarely occurring overlap of the S bead with the P-bead-associated W bead.

Intuitively, the stronger the P−S potential, which results from higher values of α_{PS} and K_{PS}, the more P beads are associated with S beads for longer times, which implies a lower degree of dissociation β. We characterize the P−S potential by reproducing the experimentally derived degree of dissociation β at the given initial acid concentration at 0.05 M, or ∼82.5%, as calculated by eq 4. It is found that, with the P−S potential well of $E_M = -4.2kT$, the simulated degree of dissociation agrees well with the experimental derived value. In order to examine whether the obtained P−S potential properly characterizes the proton equilibrium between the S bead and the surrounding W beads, we predict the degree of dissociation at several different concentrations in the dilute region without future adjustment of P−S parameters. As the concentration of sulfonate in the system increases, the degree of dissociation naturally declines. Figure 5 shows the dependence of β on the total molarity using the parameters obtained at 0.05 M ($\alpha_{PS} = 2$ and $K_{PS} = 18.5$), which gives practically exact agreement with eq 4 for the entire concentration range up to 0.1 M. The validity of eq 4 is

DOI: 10.1021/acs.jctc.5b00467
J. Chem. Theory Comput. 2015, 11, 4395−4403

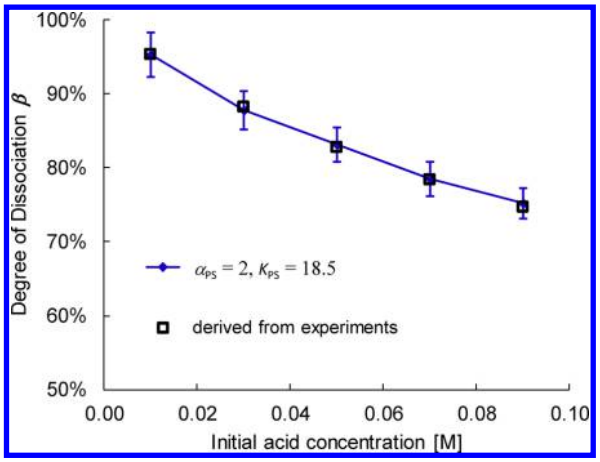

Figure 5. Degree of dissociation versus molarities of 0.01−0.1 M. Experimentally derived values are marked by squares. Lines are obtained from the DPD simulation with the Morse potential parameters fitted to reproduce the degree of dissociation at 0.05 M.

questionable at higher concentrations, because it implies that the water concentration remains constant. Good agreement between the theoretical and simulated degrees of dissociation confirms that the proposed model mimics the essence of the process. The model can be parametrized from the dissociation constant only and then applied at different concentrations. The reaction constant is mostly determined by the P−S potential well. The value of $E^M = -4.2kT$ that has been used in this particular example can be obtained by different combinations of α_{PS} and K_{PS}, the potential profile and influence on the degree of dissociation are discussed in Section S5 in the Supporting Information.

VI. CONCLUSIONS

We suggest a coarse-grained model of the proton transfer that allows for the incorporation of protonating compounds directly into the DPD force field. We introduce a new bead type that represents the proton that can be associated with base beads. The proton bead P interacts with base beads via dissociative, short-range Morse-type bonds. Base beads represent either neutral solvent (water W) or charged acid anions (sulfonate S). Protonation−deprotonation of bases is effectively modeled as a reversible reaction that occurs naturally in the course of DPD simulation. In a close analogy with the atomistic representation of protonation, the reaction proceeds via formation of an intermediate complex B_1-P-B_2 (B = S or W), where the proton is simultaneously bound with two base beads. An unavoidable breakup of the intermediate complex results in a successful or failed attempt of the proton transfer between the bases. In the case when the base beads represent individual water molecules, the intermediate complex W−P−W effectively mimics the Zundel ion. With a proper choice of the Morse potential parameters, we are able to reproduce the O−O and O−H distances in the Zundel complex in DPD simulations. Proton motion in DPD simulation consists of a sequence of distinct transfers between the neighboring base beads, imitating the Grotthuss mechanism of proton diffusion.

The short-range dissociable potentials preserve the computational efficiency of DPD and may be easily implemented in standard DPD codes. In this work, we used DL_MESO, which is an openly distributed code that allows for the implementation of smeared charges. The Morse potential that is cut and shifted within one bead diameter does not compromise the computational advantages of DPD simulations. In order to monitor the detailed transfer of P beads, the physical unit of simulation time used in this work is relatively smaller than in regular DPD simulations,[24] which causes an insignificant increase in computational costs.

The proposed model successfully describes the equilibrium between dissociated and nondissociated forms of a common organic acid of a moderate strength exemplified by benzenesulfonic acid. The potential parameters quantitatively predict the degree of dissociation at several concentrations in dilute and semidilute solutions. At the same time, the model is capable of reproducing the experimental ratio of proton and water self-diffusion coefficients, as well as the proton hopping frequency under ambient conditions. We specifically studied the models with different degrees of coarse graining corresponding to one and three water molecules per bead.

Incorporation of dissociable bonds expands the DPD method to a new class of systems with chemical equilibria. The proposed model can be suitable for modeling proton conductivity and ion-exchange reactions in solid electrolyte membranes like Nafion, for example, by embedding it directly into explicit charge DPD models suggested for Nafion segregation (see, e.g., ref 3d). Certain difficulties may be expected in applying this model to complex environments. For example, the activation energy for proton transfer in hydrated polyelectrolytes may differ substantially from that in the water bulk[27a] and be dependent on fine details of the structure, such as arrangement of surrounding anions.[27b,30] Such fine features are difficult to reproduce in DPD. On the other hand, a very reasonable agreement with experiment was obtained in recent simulations reported by Jorn and Voth,[3a] where proton diffusion in Nafion was modeled implicitly in a segregated structure obtained by DPD and electrostatic field created by the sulfonate groups. In this paper, we demonstrate the capabilities of the proposed model on a particular simple protonation reaction, however, a similar scheme can be elaborated for other equilibrium reactions sensitive to the solvent composition, which involve ion dissociation and complexation.

■ ASSOCIATED CONTENT

Supporting Information

The Supporting Information is available free of charge on the ACS Publications website at DOI: 10.1021/acs.jctc.5b00467.

Descriptions of the influence of the charge smearing on the structure of model DPD electrolytes (Section S1), the conversion of DPD time units to physical time (Section S2), the geometry of benzene−sulfonic acid−water complexes obtained from *ab initio* minimization (Section S3), and the calculations of the degree of dissociation of benzenesulfonic acid in aqueous solution (Section S4), as well as a general analysis of the influence of Morse parameters on the dissociation equilibrium of protons (Section S5) (PDF)

■ AUTHOR INFORMATION

Corresponding Author

*E-mail: aneimark@rutgers.edu.

Notes

The authors declare no competing financial interest.

DOI: 10.1021/acs.jctc.5b00467
J. Chem. Theory Comput. 2015, 11, 4395−4403

■ ACKNOWLEDGMENTS

The authors acknowledge feedback from the CECAM DPD workshop, and they thank Dr. Minerva Gonzalez-Melchor, for her advice on the smeared charge model, and Dr. Michael Seaton, for his help with the implementation of the proposed model of proton transfer into the DL_MESO open source software. This work is supported by NSF Grant No. DMR-1207239 and DTRA Grant No. HDTRA1-14-1-0015.

■ REFERENCES

(1) Hoogerbrugge, P. J.; Koelman, J. Simulating Microscopic Hydrodynamic Phenomena with Dissipative Particle Dynamics. *Europhys. Lett.* **1992**, *19* (3), 155−160.

(2) (a) Vishnyakov, A.; Talaga, D. S.; Neimark, A. V. DPD Simulation of Protein Conformations: From α-Helices to β-Structures. *J. Phys. Chem. Lett.* **2012**, *3* (21), 3081−3087. (b) Wang, Y.-L.; Lu, Z.-Y.; Laaksonen, A. Specific binding structures of dendrimers on lipid bilayer membranes. *Phys. Chem. Chem. Phys.* **2012**, *14* (23), 8348−8359. (c) Ibergay, C.; Malfreyt, P.; Tildesley, D. J. Electrostatic Interactions in Dissipative Particle Dynamics: Toward a Mesoscale Modeling of the Polyelectrolyte Brushes. *J. Chem. Theory Comput.* **2009**, *5* (12), 3245−3259.

(3) (a) Jorn, R.; Voth, G. A. Mesoscale Simulation of Proton Transport in Proton Exchange Membranes. *J. Phys. Chem. C* **2012**, *116* (19), 10476−10489. (b) Posel, Z.; Limpouchova, Z.; Sindelka, K.; Lisal, M.; Prochazka, K. Dissipative Particle Dynamics Study of the pH-Dependent Behavior of Poly(2-vinylpyridine)-block-poly(ethylene oxide) Diblock Copolymer in Aqueous Buffers. *Macromolecules* **2014**, *47* (7), 2503−2514. (c) Sindelka, K.; Limpouchova, Z.; Lisal, M.; Prochazka, K. Dissipative Particle Dynamics Study of Electrostatic Self-Assembly in Aqueous Mixtures of Copolymers Containing One Neutral Water-Soluble Block and One Either Positively or Negatively Charged Polyelectrolyte Block. *Macromolecules* **2014**, *47* (17), 6121−6134. (d) Vishnyakov, A.; Neimark, A. V. Self-Assembly in Nafion Membranes upon Hydration: Water Mobility and Adsorption Isotherms. *J. Phys. Chem. B* **2014**, *118* (38), 11353−11364.

(4) (a) Yamamoto, S.; Hyodo, S. A. A computer simulation study of the mesoscopic structure of the polyelectrolyte membrane Nafion. *Polym. J.* **2003**, *35* (6), 519−527. (b) Kyrylyuk, A. V.; Fraaije, J. Microphase separation of weakly charged block polyelectrolyte solutions: Donnan theory for dynamic polymer morphologies. *J. Chem. Phys.* **2004**, *121* (6), 2806−2812.

(5) Gonzalez-Melchor, M.; Mayoral, E.; Velazquez, M. E.; Alejandre, J. Electrostatic interactions in dissipative particle dynamics using the Ewald sums. *J. Chem. Phys.* **2006**, *125* (22), 22410710.1063/1.2400223.

(6) Groot, R. D. Electrostatic interactions in dissipative particle dynamics—Simulation of polyelectrolytes and anionic surfactants. *J. Chem. Phys.* **2003**, *118* (24), 11265−11277.

(7) Español, P.; Revenga, M. Smoothed dissipative particle dynamics. *Phys. Rev. E: Stat. Phys., Plasmas, Fluids, Relat. Interdiscip. Top.* **2003**, *67* (2), 026705 10.1103/PhysRevE.67.026705.

(8) (a) Kreuer, K. D.; Schuster, M.; Obliers, B.; Diat, O.; Traub, U.; Fuchs, A.; Klock, U.; Paddison, S. J.; Maier, J. Short-side-chain proton conducting perfluorosulfonic acid ionomers: Why they perform better in PEM fuel cells. *J. Power Sources* **2008**, *178* (2), 499−509. (b) Zawodzinski, T. A.; Neeman, M.; Sillerud, L. O.; Gottesfeld, S. Determination of Water Diffusion-Coefficients in Perfluorosulfonate Ionomeric Membranes. *J. Phys. Chem.* **1991**, *95* (15), 6040−6044.

(9) (a) Allahyarov, E.; Taylor, P. L.; Lowen, H. Simulation study of field-induced morphological changes in a proton-conducting ionomer. *Phys. Rev. E* **2010**, *81* (3), 11. (b) Schmitt, U. W.; Voth, G. A. Multistate empirical valence bond model for proton transport in water. *J. Phys. Chem. B* **1998**, *102* (29), 5547−5551. (c) Walbran, S.; Kornyshev, A. A. Proton transport in polarizable water. *J. Chem. Phys.* **2001**, *114* (22), 10039−10048. (d) Dokmaisrijan, S.; Spohr, E. MD simulations of proton transport along a model Nafion surface decorated with sulfonate groups. *J. Mol. Liq.* **2006**, *129* (1−2), 92−100.

(10) (a) Lisal, M.; Brennan, J. K.; Smith, W. R. Mesoscale simulation of polymer reaction equilibrium: Combining dissipative particle dynamics with reaction ensemble Monte Carlo. I. Polydispersed polymer systems. *J. Chem. Phys.* **2006**, *125* (16), 164905 10.1063/1.2359441. (b) Lisal, M.; Brennan, J. K.; Smith, W. R. Mesoscale simulation of polymer reaction equilibrium: Combining dissipative particle dynamics with reaction ensemble Monte Carlo. II. Supramolecular diblock copolymers. *J. Chem. Phys.* **2009**, *130* (10), 104902 10.1063/1.3079139.

(11) (a) Selvan, M. E.; Keffer, D. J.; Cui, S. Reactive Molecular Dynamics Study of Proton Transport in Polymer Electrolyte Membranes. *J. Phys. Chem. C* **2011**, *115* (38), 18835−18846. (b) Selvan, M. E.; Keffer, D. J.; Cui, S.; Paddison, S. J. A Reactive Molecular Dynamics Algorithm for Proton Transport in Aqueous Systems. *J. Phys. Chem. C* **2010**, *114* (27), 11965−11976. (c) Esai Selvan, M.; Keffer, D. J.; Cui, S.; Paddison, S. J. Proton transport in water confined in carbon nanotubes: A reactive molecular dynamics study. *Mol. Simul.* **2010**, *36* (7−8), 568−578.

(12) Karimi-Varzaneh, H. A.; Carbone, P.; Müller-Plathe, F. Fast dynamics in coarse-grained polymer models: The effect of the hydrogen bonds. *J. Chem. Phys.* **2008**, *129* (15), 154904 10.1063/1.2993111.

(13) Pike, D. Q.; Detcheverry, F. A.; Muller, M.; de Pablo, J. J. Theoretically informed coarse grain simulations of polymeric systems. *J. Chem. Phys.* **2009**, *131* (8), 084903 10.1063/1.3187936.

(14) Nikoubashman, A.; Register, R. A.; Panagiotopoulos, A. Z. Sequential Domain Realignment Driven by Conformational Asymmetry in Block Copolymer Thin Films. *Macromolecules* **2014**, *47* (3), 1193−1198.

(15) Vishnyakov, A.; Lee, M. T.; Neimark, A. V. Prediction of the Critical Micelle Concentration of Nonionic Surfactants by Dissipative Particle Dynamics Simulations. *J. Phys. Chem. Lett.* **2013**, *4* (5), 797−802.

(16) Groot, R. D.; Warren, P. B. Dissipative particle dynamics: Bridging the gap between atomistic and mesoscopic simulation. *J. Chem. Phys.* **1997**, *107* (11), 4423−4435.

(17) Español, P.; Warren, P. Statistical-Mechanics of Dissipative Particle Dynamics. *Europhys. Lett.* **1995**, *30* (4), 191−196.

(18) Groot, R. D. Erratum: "Electrostatic interactions in dissipative particle dynamics—Simulation of polyelectrolytes and anionic surfactants" [*J. Chem. Phys.* 118, 11265 (2003)]. *J. Chem. Phys.* **2003**, *119* (19), 10454.

(19) Warren, P. B.; Masters, A. J. Phase behaviour and the random phase approximation for ultrasoft restricted primitive models. *J. Chem. Phys.* **2013**, *138* (7), 07490110.1063/1.4791635.

(20) Warren, P. B.; Vlasov, A. Screening properties of four mesoscale smoothed charge models, with application to dissipative particle dynamics. *J. Chem. Phys.* **2014**, *140* (8), 08490410.1063/1.4866375.

(21) Ewald, P. P. Evaluation of optical and electrostatic lattice potentials (in Ger.). *Ann. Phys.* **1921**, *64*, 253.

(22) Seaton, M. A.; Anderson, R. L.; Metz, S.; Smith, W. DL_MESO: Highly scalable mesoscale simulations. *Mol. Simul.* **2013**, *39* (10), 796−821.

(23) (a) Hofmann, D. W. M.; Kuleshova, L.; D'Aguanno, B. A new reactive potential for the molecular dynamics simulation of liquid water. *Chem. Phys. Lett.* **2007**, *448* (1−3), 138−143. (b) Hofmann, D. W. M.; Kuleshova, L.; D'Aguanno, B. Molecular dynamics simulation of hydrated Nafion with a reactive force field for water. *J. Mol. Model.* **2008**, *14* (3), 225−235.

(24) Groot, R. D.; Rabone, K. L. Mesoscopic simulation of cell membrane damage, morphology change and rupture by nonionic surfactants. *Biophys. J.* **2001**, *81* (2), 725−736.

(25) (a) Choi, P.; Jalani, N. H.; Datta, R. Thermodynamics and proton transport in Nafion—II. Proton diffusion mechanisms and conductivity. *J. Electrochem. Soc.* **2005**, *152* (3), E123−E130. (b) Kornyshev, A. A.; Kuznetsov, A. M.; Spohr, E.; Ulstrup, J.

DOI: 10.1021/acs.jctc.5b00467
J. Chem. Theory Comput. 2015, 11, 4395−4403

Kinetics of proton transport in water. *J. Phys. Chem. B* **2003**, *107* (15), 3351−3366.
(26) Jeffrey, G. *An Introduction to Hydrogen Bonding*; Oxford University Press: New York, 1997; p 12.
(27) (a) Cappadonia, M.; Erning, J. W.; Stimming, U. Proton Conduction of Nafion-117 Membrane between 140 K and Room-Temperature. *J. Electroanal. Chem.* **1994**, *376* (1−2), 189−193. (b) Eikerling, M.; Kornyshev, A. A.; Spohr, E. Proton-Conducting Polymer Electrolyte Membranes: Water and Structure in Charge. In *Fuel Cells I*; Scherer, G. G., Ed.; Advances in Polymer Science, Vol. *215*; Springer: Berlin, Heidelberg, Germany, 2008; pp 15−5410.1007/12_2008_132. (c) Spohr, E.; Commer, P.; Kornyshev, A. A. Enhancing proton mobility in polymer electrolyte membranes: Lessons from molecular dynamics simulations. *J. Phys. Chem. B* **2002**, *106* (41), 10560−10569.
(28) Klamt, A.; Schuurmann, G. COSMO—A New Approach to Dielectric Screening in Solvents with Explicit Expressions for the Screening Energy and Its Gradient. *J. Chem. Soc., Perkin Trans. 2* **1993**, No. 5, 799−805.
(29) Pulay, P.; Baker, J.; Wolinski, K. *PQS*, version 4.0; Parallel Quantum Solutions: Fayetteville, AR, 1997; http://www.pqs-chem.com.
(30) (a) Roudgar, A.; Narasimachary, S. P.; Eikerling, M. *Ab initio* study of surface-mediated proton transfer in polymer electrolyte membranes. *Chem. Phys. Lett.* **2008**, *457* (4−6), 337−341. (b) Ioselevich, A. S.; Kornyshev, A. A.; Steinke, J. H. G. Fine morphology of proton-conducting ionomers. *J. Phys. Chem. B* **2004**, *108* (32), 11953−11963.

DOI: 10.1021/acs.jctc.5b00467
J. Chem. Theory Comput. 2015, 11, 4395−4403